# Estimation of Spectral Abundance Fractions using Fixed Acceleration Coefficients PSO Approach

Vaibhav Lodhi
*Advanced Technology Development Centre*
*IIT Kharagpur*
Kharagpur, India
vaibhav.lodhi@gmail.com

Debashish Chakravarty
*IIT Kharagpur*
Kharagpur, India

Pabitra Mitra
*IIT Kharagpur*
Kharagpur, India

***Abstract*—The occurrence of mixed pixels is common in hyperspectral data. It is necessary to analyse mixed pixels for classification, detection, discrimination, and quantification. Spectral unmixing is needed for mixed pixel analysis of the hyperspectral data. It includes endmember extraction and abundance estimation of mixed pixels. In this work, fixed acceleration coefficients based PSO approach is applied and analysed for abundance fractions estimation of endmembers in spectral unmixing. Time varying inertia weight strategy and fixed acceleration coefficient values have been used in this approach. For estimation, supervised linear mixing model is considered, following sum-to-one and non-negative constraints, respectively. A proposed approach is tested over real hyperspectral data i.e., jasper ridge dataset. The performance metrics of the approach are Average Abundance Error (AAE) and Root Mean Square Error (RMSE). AAE and RMSE values have been noted over different number of iterations. It is observed that result of fixed acceleration coefficients based PSO approach is promising.**

***Index Terms*—Hyperspectral Imaging, PSO, Abundance Estimation, LMM**

## I. Introduction

In recent years, hyperspectral imaging has been achieved prominent progress in hardware and software for various applications. It consists of hundreds of spectral bands with a spectral resolution of less than 2 nm to 10 nm which generates continuous spectral signature. While multispectral imaging consists of few numbers of spectral bands and comparatively less spectral resolution. Consequently, it generates a discrete spectral fingerprint of the object under test. Hyperspectral imaging has been using in various applications which includes forestry [1], vegetation and water resources [2], agriculture and food inspection [3], biomedical applications [4], oceanology [5] and geological [6] applications. However, it is noticed that the spatial resolution of the most of the hyperspectral images are low. In remote sensing, it is obvious that the pixels consist mixture of several spectral components, known as endmembers. In such a case, response of a pixel is mixture of individual response of each endmember within the pixel. Thus, the observed pixels are mixed pixels which consist spectral signature of several pure materials. The subject of mixed pixel increases as the pixel size increases. Such mixed pixels impose restrictions on the practical application of hyperspectral images. In hyperspectral imaging, many applications require estimation of abundance proportions of endmembers. The knowledge of abundance fractions is used in several applications which includes forestry, mining and others.

Therefore, segregation of the mixed pixels is known as hyperspectral unmixing which is important for interpretation of data. Spectral unmixing [7] refers to the process of separating mixed spectra into a set of constitutive spectras and their abundance fractions. The endmembers are assumed as a pure substance present in the image and abundance fractions indicate their respective percentage in the pixel. Decomposition of mixed pixel consists of two steps i.e., endmember extraction and abundance estimation. In [8], Omran et al. have used PSO for endmember selection for multispectral images. And, in [9], [10], authors have been used Particle Swarm Optimization (PSO) to perform the nonlinear unmixing operation over the hyperspectral image. However, Linear Mixing Model (LMM) is very popular in spectral unmixing. It is easy to calculate and simple in mathematical representation. In LMM, It is assumed that each pixel in the hyperspectral image is linearly weighted by the endmembers existing in the pixel. Hence, the objective of this study is to estimate the abundance fractions of hyperspectral data by exploiting the capability of fixed acceleration coefficient PSO approach. It is achieved by minimization of the objective function. Herein, it is considered that the endmembers are available and linear mixing model is used for abundance estimation operation. In this work, Average Abundance Error (AAE) and Root Mean Square Error (RMSE) have been calculated over a different number of iterations to find the optimum number of iterations for estimation purpose.

The remainder of the paper is organized in the following manner. Section 2 and 3 discuss PSO and linear mixing model as a common ground. Section 4 presented the methodology for the proposed work which includes initialization, objective function, parameters and performance measures. An experiment has been presented in section 5 which includes result and analysis. Finally, section 6 ends with the conclusion and future scopes.

## II. PSO

Particle Swarm Optimization(PSO) is a heuristic search or optimization technique inspired by birds flocking or fish schooling behavior. It is stochastic population-based optimization approach and was first introduced by Kennedy and

Eberhart in 1995 [11]. PSO is simple, robust and efficient optimization algorithm. In general, PSO minimizes the given function of several variables iteratively in order find the optimal solution. Since the commencement of PSO, it has been using in several applications which includes robotics and control [12], [13], image processing [14], [15] and others. Equations of particle for velocity and position are given in Equation 1 and 2.

$$v_i^{t+1} = w^t * v_i^t + c_1 * R_1() * (P_i^t - x_i^t) + c_2 * R_2() * (P_g^t - x_i^t) \quad (1)$$

$$x_i^{t+1} = v_i^{t+1} + x_i^t \quad (2)$$

In above equation, $i$ is the particle index, $w$ is inertia weight, $c_1$ and $c_2$ are the acceleration coefficients, and $R_1()$ and $R_2()$ are the random values. $P_i$ and $P_g$ are the personal best and global best. It is noticed that the PSO is sensitive to control parameters especially inertia weight, swarm size and acceleration coefficients. Wrong initialization of these parameters may lead to inaccurate output. Different types of time varying and fixed, acceleration coefficients and inertia weight strategies have been used to obtain accurate output. Also, other algorithmic configurations have been used for tuning these parameters.

## III. Linear Mixing Model

In remote sensing, spectral mixture analysis has been used to do classification, detection, quantification, and discrimination. In general, a pixel contains a number of materials in hyperspectral/multispectral imagery. In the past, two major mixing models have been proposed. And, they are linear mixing model (LMM) and nonlinear mixing model (NMM). LMM is simple in mathematical representation and easy to calculate. In LMM [16], mixed pixel spectra are represented as a linear combination of component spectras. And, the weight of each spectrum is proportional to the covered fractional area of the mixed pixel. The general equation for LMM is given below:

$$y = \sum_{k=1}^{M} \alpha_k x_k + e, \quad (3)$$

It follows sum-to-one and non-negative constraints, respectively, which are given below:

$$\sum_{k=1}^{M} \alpha_k = 1, \qquad \alpha_k \geq 0 \qquad \forall k = 1, ..., M. \quad (4)$$

where,

$y$ Mixed pixel spectra;
$x_k$ Endmember;
$\alpha_k$ Abundance fraction;
$M$ Number of endmembers;
$e$ Error term.

## IV. Methodology

In this section, methodology for the proposed work has been discussed. Methodology for the proposed work for abundance estimation has been shown in Figure 1. Different sections of methodology have been discussed below:

### A. Initialization

Initial velocity and position of the each particle is initialized as Random value and (1/number of endmembers)*Rand i.e., random number.

### B. Setting of Parameters

There are three parameters which are needed to adjust prior to do optimization. And, the parameters are inertia weight, social and cognitive component. Sugneo function [17] is used as an inertia weight strategy. Expression for the sugeno function is given in Equation 5.

$$w = (1 - \beta)/(1 - s\beta) \quad (5)$$

In above equation, $s$ is constant, taken as -1.5 and $\beta$ is (current iteration/maximum iteration). Fixed value of acceleration coefficients have been used for abundance estimation. Values of cognitive ($c_1$) and social ($c_2$) components are taken as 2 in the Equation 1.

### C. Personal and Global best

Schematic representation of the global best particle per pixel as shown in Figure 2. In this Figure, N represents the number of pixels and n denotes the number of particles per pixel. $P_1 ... P_n$ represent the number of particles per pixel. Value of global best changes, if the fitness function value is less than previous value of particular pixel during iteration run. Each pixel has its own global best. After fixed number of iterations run, global best per pixel represents the abundance fraction of that pixel. During the course of iterations, particles follow sum-to-one and non-negative constraints, respectively. $G_1, ...G_N$ represent the global best of $M_1, ....M_N$ pixels.

### D. Termination Criteria

In this approach, Number of iterations is the termination criteria. AAE and RMSE values are noted over 60,80, 100, 120, 140 and 160 iterations to find the optimum number of iterations number needed for solution.

### E. Objective Function

The objective function for the PSO approach has been given in Equation 6.

$$\min f_i = \sum_{i=1}^{N} (y_i - x * a_i)^2 \quad (6)$$

$y$ and $x$ represent the mixed pixels and endmembers and $a$ is the abundance vector. In above equation, $y$ and $x$ are fixed while $a$ is the optimizing one.

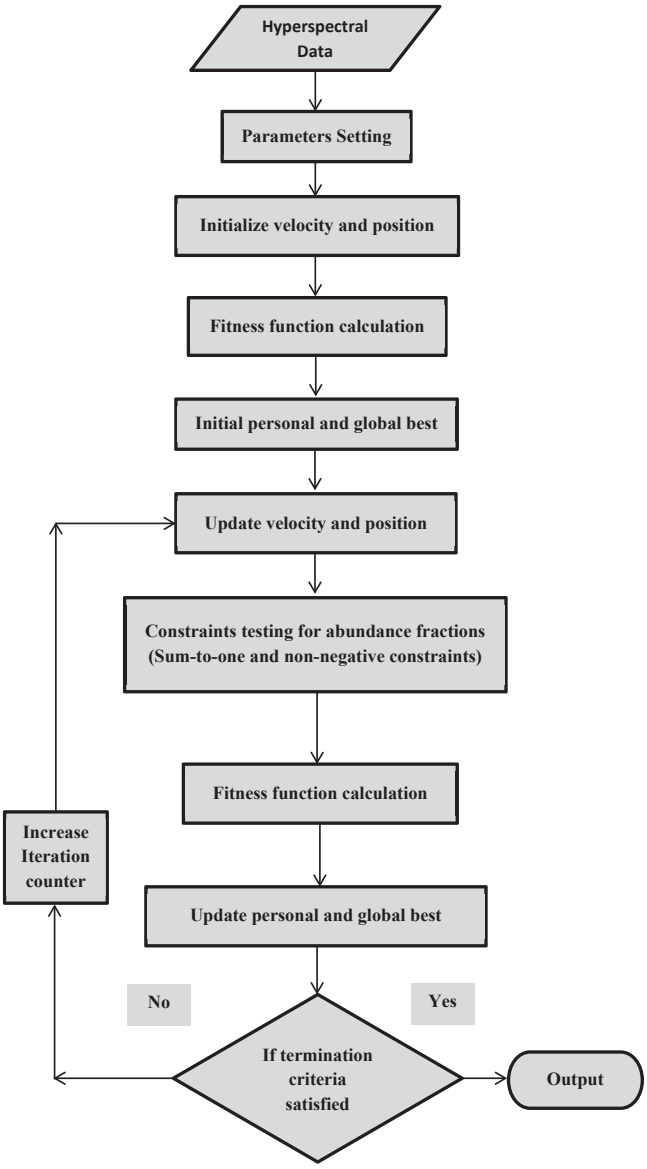


Fig. 1. Methodology for the proposed work

### F. Performance Measure

Two metrics are used to measure the performance i.e., Average Abundance Error (AAE) and Root Mean Square Error (RMSE) for spectral abundance estimation. They are calculated at different number of iterations. Expressions for the AAE and RMSE are given below:

$$AAE = \sqrt{1/(NM)\sum_{j=1}^{N}(Actual_j - Predicted_j)^2} \quad (7)$$

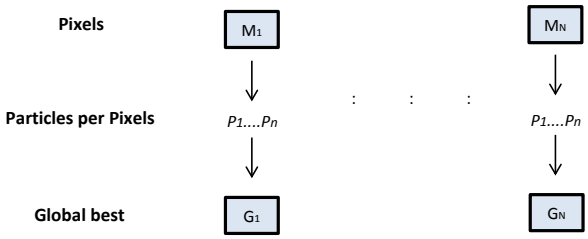


Fig. 2. Schematic representation of the global best particle per pixel

$$RMSE = \sqrt{1/N\sum_{j=1}^{N}(Actual_j - Predicted_j)^2} \quad (8)$$

In above equation, $Actual_j$ and $Predicted_j$ are the actual and estimated abundance vectors for the $j_{th}$ pixel, N is the number of pixels and M is the number of endmembers. AAE and RMSE values are recorded over different number of iterations in order to find the optimum number of iterations.

## V. Experiment

In this work, PSO approach is tested over real hyperspectral data of jasper ridge [18]–[20]. It is one of the popular hyperspectral dataset consists of 224 channels ranging from 380 nm to 2500 nm and the spectral resolution is up to 9.46 nm. After correction, it consists of 198 channels. For this work, a subpart of the corrected dataset is used for abundance estimation. There are four endmembers present in the data i.e., road, soil, water, and tree and their spectral signatures for 192 bands have been shown in Figure 3. Actual abundance fractions of the endmembers and the endmembers are given with the dataset for testing the performance.

For PSO approach, a subpart of the jasper ridge dataset has been used i.e., 4000 to 4999 pixel range (1000 pixels) along with 192 bands. Twenty-five particles per pixel have been used in order to find the abundance fractions of each endmembers. Each particle has been following sum-to-one and non-negative constraints, respectively. Position of each particle is initialized by the value i.e., ((1/number of endmembers)*Rand). It is run over different number of iterations to find the suitable iteration for convergence. AAE and RMSE values are taken over a different number of iterations as shown in Figure 4. Both values have been calculated in between the estimated and the actual(given) abundance fractions. It is observed that the value of AAE and RMSE are 0.0894 and 0.1788 at 60 iterations. After 120 iterations, it is noticed that the values of AAE and RMSE start converging. There is less variation in the value after 120 iterations. At 160 iterations, values of AAE and RMSE are 0.0776 and 0.1552. Furthermore, an accuracy of this proposed approach may be increased by

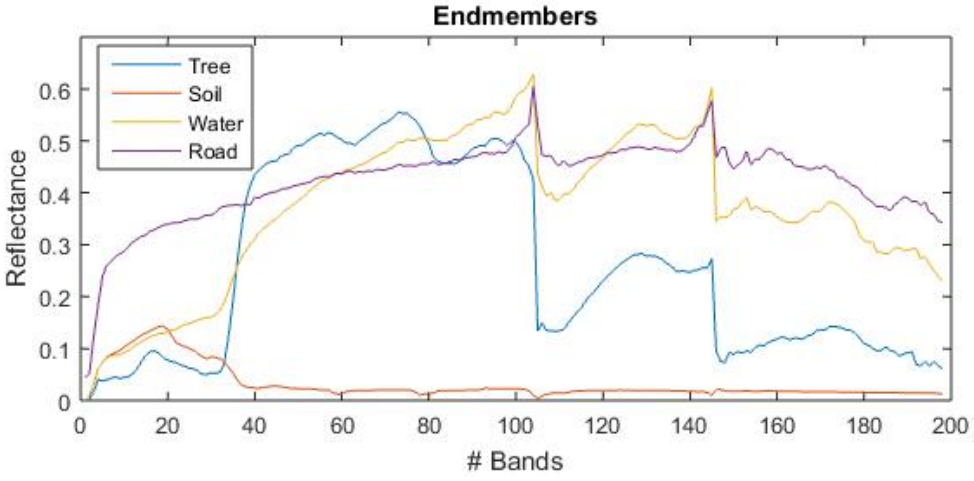


Fig. 3. Endmembers for spectral abundance estimation

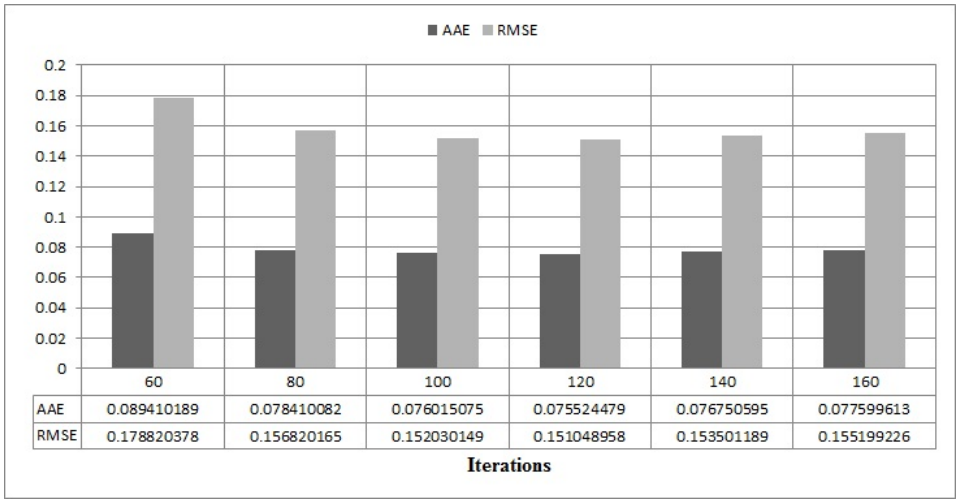


| | 60 | 80 | 100 | 120 | 140 | 160 |
|---|---|---|---|---|---|---|
| AAE | 0.089410189 | 0.078410082 | 0.076015075 | 0.075524479 | 0.076750595 | 0.077599613 |
| RMSE | 0.178820378 | 0.156820165 | 0.152030149 | 0.151048958 | 0.153501189 | 0.155199226 |

Fig. 4. AAE and RMSE for spectral abundance estimation at different iterations

tuning the parameters values, the number of particles and other parameters.

## VI. Conclusion

Spectral unmixing is one of the major post-processing operations of hyperspectral image processing. In this work, PSO based approach is applied to estimate the spectral abundance fractions by minimizing the objective function. Time varying inertia weight strategy and fixed acceleration coefficients based PSO approach is used. For abundance estimation, supervised linear mixing model is considered. It is tested over jasper ridge dataset which consists of four endmembers and actual abundance fractions have been given for testing puropose. AAE and RMSE have been calculated over different iterations and found the solution start converging after 120 (approx.) iterations. Values of AAE and RMSE at 120 iterations are 0.0755 and 0.1510, respectively. It is found that the fixed acceleration coefficients based PSO approach has a potential to compute the abundance fractions in spectral unmixing. Accuracy and efficiency of this approach may be increased by varying and tuning the different parameters and considering different mixing models.

## References

[1] D. G. Goodenough, A. Dyk, K. O. Niemann, J. S. Pearlman, H. Chen, T. Han, M. Murdoch, and C. West, "Processing hyperion and ali for forest classification," *IEEE transactions on geoscience and remote sensing*, vol. 41, no. 6, pp. 1321–1331, 2003.

[2] E. Adam, O. Mutanga, and D. Rugege, "Multispectral and hyperspectral remote sensing for identification and mapping of wetland vegetation: a review," *Wetlands Ecology and Management*, vol. 18, no. 3, pp. 281–296, 2010.

[3] R. Lu and Y.-R. Chen, "Hyperspectral imaging for safety inspection of food and agricultural products," in *Pathogen Detection and Remediation for Safe Eating*, vol. 3544. International Society for Optics and Photonics, 1999, pp. 121–134.

[4] M. E. Martin, M. B. Wabuyele, K. Chen, P. Kasili, M. Panjehpour, M. Phan, B. Overholt, G. Cunningham, D. Wilson, R. C. DeNovo *et al.*, "Development of an advanced hyperspectral imaging (hsi) system with applications for cancer detection," *Annals of biomedical engineering*, vol. 34, no. 6, pp. 1061–1068, 2006.

[5] A. A. Gitelson, B.-C. Gao, R.-R. Li, S. Berdnikov, and V. Saprygin, "Estimation of chlorophyll-a concentration in productive turbid waters using a hyperspectral imager for the coastal oceanthe azov sea case study," *Environmental Research Letters*, vol. 6, no. 2, p. 024023, 2011.

[6] F. D. Van der Meer, H. M. Van der Werff, F. J. Van Ruitenbeek, C. A. Hecker, W. H. Bakker, M. F. Noomen, M. Van Der Meijde, E. J. M. Carranza, J. B. De Smeth, and T. Woldai, "Multi-and hyperspectral geologic remote sensing: A review," *International Journal of Applied Earth Observation and Geoinformation*, vol. 14, no. 1, pp. 112–128, 2012.

[7] N. Keshava and J. F. Mustard, "Spectral unmixing," *IEEE signal processing magazine*, vol. 19, no. 1, pp. 44–57, 2002.

[8] M. Omran, A. P. Engelbrecht, and A. Salman, "A pso-based end-member selection method for spectral unmixing of multispectral satellite images," *International Journal of Computational Intelligence*, vol. 2, pp. 1304–4508, 2005.

[9] L. Zhong, W. Luo, and L. Gao, "A particle swarm optimization algorithm for unmixing the polynomial post-nonlinear mixing model," in *Image and Signal Processing, BioMedical Engineering and Informatics (CISP-BMEI), International Congress on*. IEEE, 2016, pp. 596–600.

[10] ——, "Particle swarm optimization for nonlinear spectral unmixing: A case study of generalized bilinear model," in *Natural Computation, Fuzzy Systems and Knowledge Discovery (ICNC-FSKD), 2016 12th International Conference on*. IEEE, 2016, pp. 211–217.

[11] J. Kennedy, "Particle swarm optimization," in *Encyclopedia of machine learning*. Springer, 2011, pp. 760–766.

[12] M. Dadgar, S. Jafari, and A. Hamzeh, "A pso-based multi-robot cooperation method for target searching in unknown environments," *Neurocomputing*, vol. 177, pp. 62–74, 2016.

[13] Y. Cai and S. X. Yang, "An improved pso-based approach with dynamic parameter tuning for cooperative multi-robot target searching in complex unknown environments," *International Journal of Control*, vol. 86, no. 10, pp. 1720–1732, 2013.

[14] M. Maitra and A. Chatterjee, "A hybrid cooperative–comprehensive learning based pso algorithm for image segmentation using multilevel thresholding," *Expert Systems with Applications*, vol. 34, no. 2, pp. 1341–1350, 2008.

[15] A. N. Benaichouche, H. Oulhadj, and P. Siarry, "Improved spatial fuzzy c-means clustering for image segmentation using pso initialization, mahalanobis distance and post-segmentation correction," *Digital Signal Processing*, vol. 23, no. 5, pp. 1390–1400, 2013.

[16] D. Manolakis, C. Siracusa, and G. Shaw, "Hyperspectral subpixel target detection using the linear mixing model," *IEEE Transactions on Geoscience and Remote Sensing*, vol. 39, no. 7, pp. 1392–1409, 2001.

[17] K. Lei, Y. Qiu, and Y. He, "A new adaptive well-chosen inertia weight strategy to automatically harmonize global and local search ability in particle swarm optimization," in *Systems and Control in Aerospace and Astronautics, 2006. ISSCAA 2006. 1st International Symposium on*. IEEE, 2006, pp. 4–pp.

[18] F. Zhu, Y. Wang, B. Fan, G. Meng, and C. Pan, "Effective spectral unmixing via robust representation and learning-based sparsity," *arXiv preprint arXiv:1409.0685*, 2014.

[19] F. Zhu, Y. Wang, B. Fan, S. Xiang, G. Meng, and C. Pan, "Spectral unmixing via data-guided sparsity," *IEEE Transactions on Image Processing*, vol. 23, no. 12, pp. 5412–5427, 2014.

[20] F. Zhu, Y. Wang, S. Xiang, B. Fan, and C. Pan, "Structured sparse method for hyperspectral unmixing," *ISPRS Journal of Photogrammetry and Remote Sensing*, vol. 88, pp. 101–118, 2014.